Strong FEM Calculation of the Influence of the Conductor's Position on Quasi-Static Parameters of the Shielded Stripline With Anisotropic Dielectric

Žaklina J.Mančić[1] Vladimir V. Petrović[2]

Abstract – **Strong formulation of the Finite Element Method is applied for calculation of effective permittivity and characteristic impedance of asymmetric shielded stripline filled with anisotropic dielectric. The influence of the position of the strip conductor is studied for two typical anisotropic substrates — sapphire and boron nitride. Rectangular elements of the third degree are applied.**

Keywords – **Anisotropic dielectric, asymmetric stripline, shielded stripline, strong FEM formulation.**

I. Introduction

TEM transmission lines with anisotropic dielectric cannot be easily analyzed by the Method of Moments, even when dielectric is homogeneous and linear. In these cases Finite Element Method (FEM) [1, 2] is a very good choice. It was shown that strong FEM formulation of the Galerkin type [3,4] can be successfully applied to 2-D closed electrostatic problems for both isotropic [4, 5] and anisotropic [6, 7] dielectrics.

In this paper strong FEM formulation is applied for calculation of quasi-static parameters of the shielded asymmetric stripline with homogeneous anisotropic dielectric.

II. Basic FEM Methodology for Anisotropic Media

Consider a 2-D calculation domain, as shown in Fig.1. Starting for differential equation for electrostatic potential,

$$\mathrm{div}_S(\overline{\overline{\varepsilon}}\,\mathrm{grad}_S V) = 0\,, \tag{1}$$

where div_S is a surface divergence, grad_S is a surface gradient and $\overline{\overline{\varepsilon}}$ is a diagonal 2×2 permittivity tensor, $\overline{\overline{\varepsilon}} = \mathrm{diag}[\varepsilon_{xx}\ \varepsilon_{yy}]$. Calculation domain is divided into M subdomains (elements) and approximate solution for $V(x,y)$ presented as a linear combination of basis functions, $V \approx f = \sum_{j=1}^{N} a_j f_j$, where a_j are unknown coefficients. In this analysis rectangular elements are applied. Every basis function is nonzero on the surface of one element (for singlet functions) or on several neighboring elements (for doublet and quadruplet functions) [4, 6, 7]. According to Galerkin's procedure [1, 2], a system of linear algebraic equations is formed,

$$[K_{ij}][a_j] = [G_i]\,, \qquad i, j = 1,\ldots, N\,, \tag{2}$$

$$K_{ij} = \int_S (\mathrm{grad}\, f_i)\left(\overline{\overline{\varepsilon}}\,\mathrm{grad}\, f_j\right)\mathrm{d}S\,, \qquad G_i = \int_{C_2} f_i\, D_{n0}\,\mathrm{d}l\,, \tag{3}$$

where D_{n0} is the given normal component of vector $\mathbf{D}$ on contour C_2, i and j are global indices of basis functions, S is the surface of the calculation domain, $S = \bigcup_{e=1}^{M} S^e$, and S^e is the surface of the e-th element. By solving (2), unknown coefficients a_j are obtained, and, thus, the approximate distribution of potential *V*.

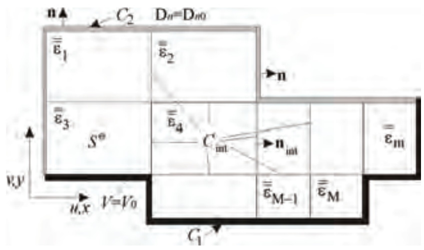

Fig. 1. Two-dimensional calculation domain divided into elements.

III. Strong FEM Basis Functions

In [3] strong FEM formulation for 1-D electromagnetic (EM) problems is introduced by the use of special, C^1 continuous, basis functions (strong basis functions). In corresponding formulation for 2-D electrostatic problems [4, 5] strong 2-D basis functions automatically satisfy continuity of potential V (C^0 continuity) and continuity of D_n (generalized C^1 continuity) on interelement boundaries (C_{int} in Fig.1). Complete set of strong basis functions for 2-D problems in homogeneous (isotropic or anisotropic) media consists of four types of quadruplets (Fig.2), two types of doublets (Fig.3) and various singlets (Fig.4).

[1]Žaklina Mančić is with the Faculty of Electronic Engineering, Aleksandra Medvedeva 14, 18000 Nis, Serbia, E-mail: zaklina.mancic@elfak.ni.ac.rs.

[2]Vladimir Petrović is with the School of Electrical Engineering Belgrade, Bulevar kralja Aleksandra 73, 11120 Belgrade, Serbia, E-mail: vp@etf.bg.ac.rs.

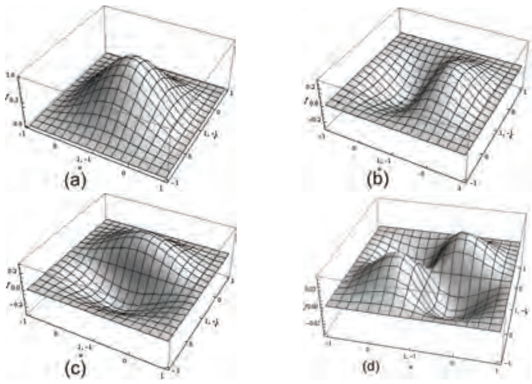

Fig. 2. Quadruplets for the strong FEM formulation. They provide continuity of (a) V , (b) D_{nx} , (c) D_{ny} , and (d) both D_{nx} and D_{ny} .

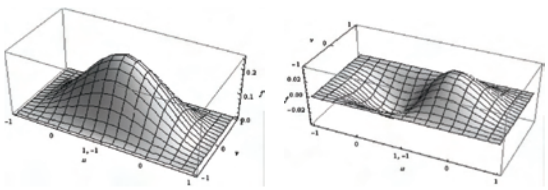

Fig. 3. Doublets for the strong FEM formulation.

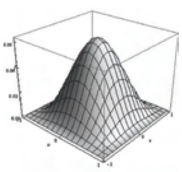

Fig. 4. Typical singlet for the strong FEM formulation.

IV. NUMERICAL RESULTS

Two geometries, depicted in Fig.5 and Fig.11, are considered. Although formally the same, the two geometries differ in orientation (horizontal and vertical) of the strip. Two typical anisotropic substrates for planar transmission lines are considered. The first is sapphire ($\varepsilon_{rxx} = 9.4, \varepsilon_{ryy} = 11.6$), and the second is boron nitride, ($\varepsilon_{rxx} = 5.12, \varepsilon_{ryy} = 3.4$). Effective relative permittivity, ε_{re}, and characteristic impedance, Z_c, were calculated by standard formulas for non-magnetic dielectrics, $\varepsilon_{re} = C'/C'_0$ and $Z_c = \left(c_0\sqrt{C'C'_0}\right)^{-1}$, where C' is the capacitance per unit length of the analyzed line, C'_0 is its capacitance per unit length when dielectric is replaced by vacuum, and c_0 is the speed of light in free-space. Capacitances per unit length were calculated by the use of energy formula,

$$W' = \frac{1}{2}C'U^2 = \sum_e \int_{S^e} w_e \mathrm{d}S = \frac{1}{2}\sum_e \int_{S^e} \mathbf{E}\cdot\mathbf{D}\mathrm{d}S, \quad \mathbf{E} = -\operatorname{grad}V$$

We used $N = 512$ elements of the third order in both *x*- and *y*-directions ($n_x = n_y = 3$). The third-order elements represent the lowest-order approximation for the strong FEM formulation [4].

IV.A. Example 1

For the stripline whose cross-section is given in Fig.5, the strip is parallel to the wider side of the rectangular shield. Relative dimensions of the line are chosen as: $a/b = 3$, $w/b = 1$, $t/b = 0.1$, while h/b and s/b are variable.

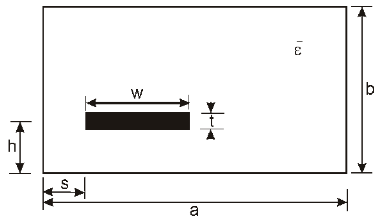

Fig. 5. Geometry of the first analyzed structure.

In Figs.6 and 7 relative effective permittivity, ε_{re}, and characteristic impedance, Z_c, are presented for sapphire, and in Figs. 8 and 9, the same parameters are presented for boron nitride. In Fig.10, field lines for sapphire, $h/b = 0.45$, $s/b = 0.5$ are depicted (by the use of the commercial software [8]).

From those four diagrams it can be seen that ε_{re} and Z_c are changing rapidly when the strip is close to the shield. When the strip is relatively far from the shield, these parameters are changing slowly.

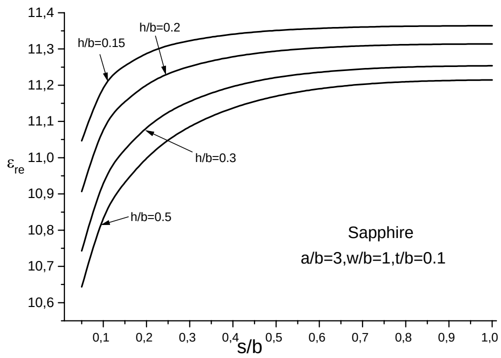

Fig. 6. Effective relative permittivity of the shielded stripline filled with sapphire, as a function of s/b .

From Figs.6 and 8 can be seen that when the strip approaches the wall of the shield, ε_{re} tends to values closer to ε_{rxx} . This can be explained by the edge effect in which the *x*-component of the field is dominant. When the strip moves away from the wall towards the center of the structure, the *y*-component of the field relatively increases (compared to the *x*-component), and ε_{re} tends to values closer to ε_{ryy} . When the strip is closer to the bottom of the structure, ε_{re} tends to values closer to ε_{ryy} , as the *y*-component of the field then increases even more. The sketch of electric field lines, shown in Fig.10, can help for visual illustrations of these effects.

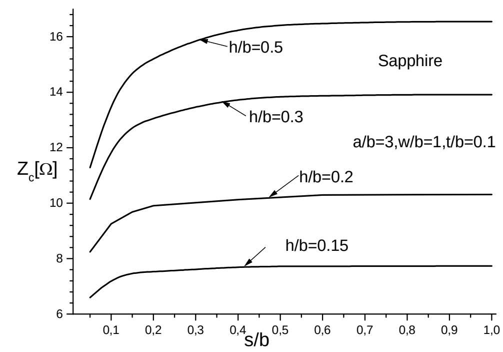

Fig. 7. Characteristic impedance of the shielded stripline filled with sapphire, as a function of s/b.

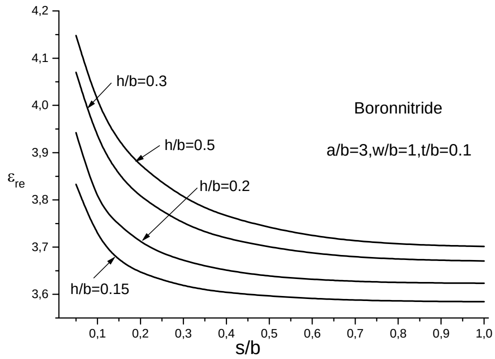

Fig. 8. Effective relative permittivity of the shielded stripline filled with boron nitride, as a function of s/b.

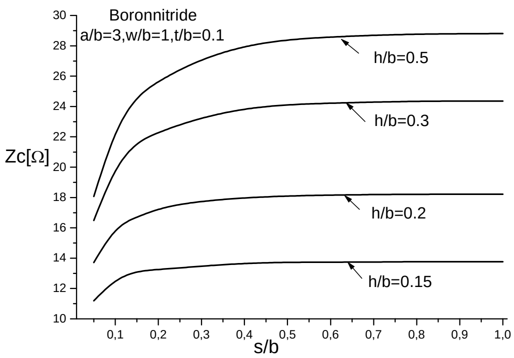

Fig. 9. Characteristic impedance of the shielded stripline filled with boron nitride, as a function of s/b.

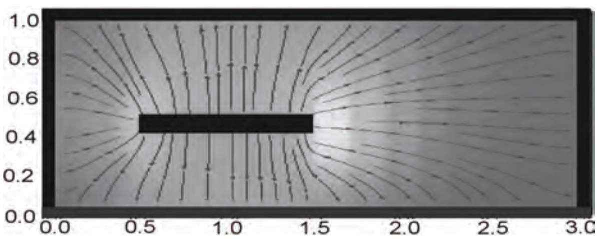

Fig. 10 Electric field lines for sapphire ($a/b = 3$, $w/b = 1$, $t/b = 0.1$, $h/b = 0.45$, $s/b = 0.5$).

As for the characteristic impedance, in all cases it increases with moving the strip away from the shield towards the center of the structure. This is due to decrease of the capacitance per unit length and is not directly associated with anisotropic characteristics of the substrate.

IV.B. Example 2

For the stripline whose cross-section is given in Fig.11, the strip is parallel to the narrower side of the rectangular shield. Relative dimensions of the line are chosen as: $a/b = 3$, $w/b = 0.5$, $t/b = 0.1$, while h/b and s/b are variable.

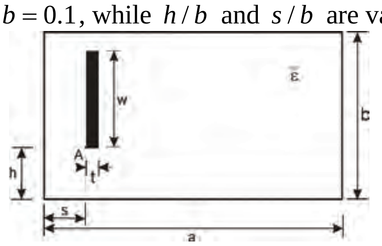

Fig. 11. Geometry of the second analyzed structure.

In Figs.12 and 13 relative effective permittivity, ε_{re}, and characteristic impedance, Z_c, are presented for sapphire, and in Figs. 14 and 15, the same parameters are presented for boron nitride. In Fig.16, field lines for sapphire, $h/b = 0.45$, $s/b = 0.5$ are depicted (by the use of the commercial software [8]).

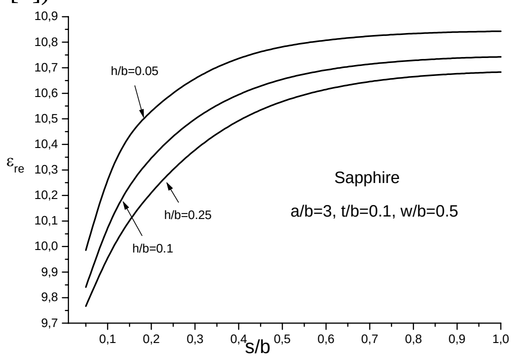

Fig. 12. Effective relative permittivity of the shielded stripline filled with sapphire, as a function of s/b.

Those diagrams practically illustrate the same effects as in example 1.

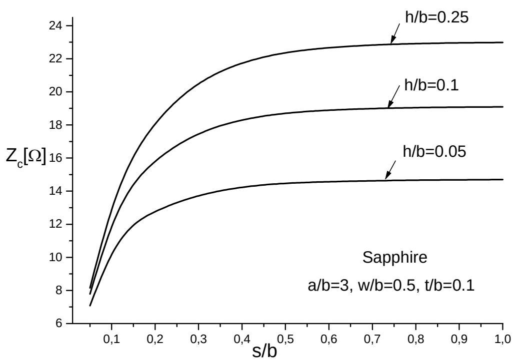

Fig. 13. Characteristic impedance of the shielded stripline filled with sapphire, as a function of s/b.

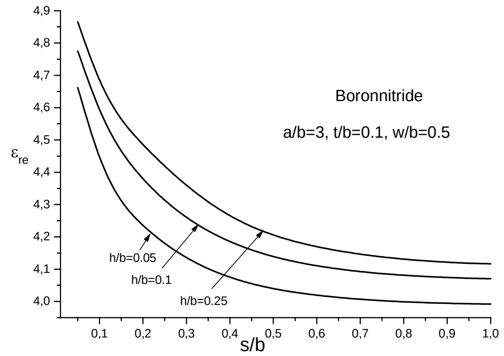

Fig. 14. Effective relative permittivity of the shielded stripline filled with boron nitride, as a function of s/b.

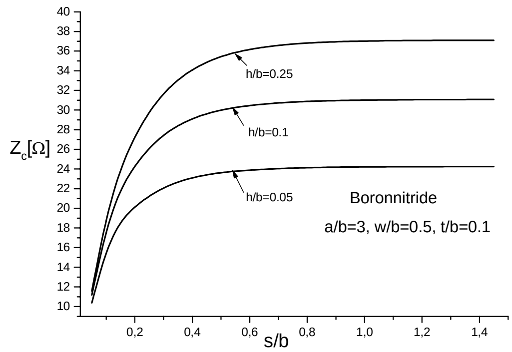

Fig. 15. Characteristic impedance of the shielded stripline filled with boron nitride, as a function of s/b.

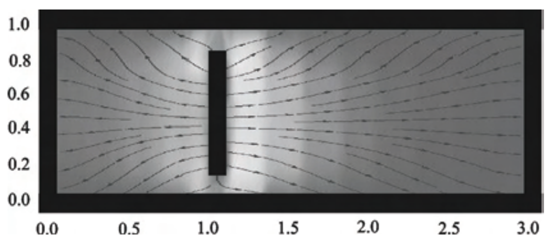

Fig. 16. Electric field lines for sapphire ($h/b = 0.1$, $s/b = 1$, $a/b = 3$, $t/b = 0.1$, $w/b = 0.8$).

V. Conclusion

Quasi-static parameters of asymmetric shielded stripline, are obtained by the strong FEM formulation for various positions of the strip. It was shown that effective relative permittivity of the stripline tends to values closer to ε_{rxx} when the strip moves closer to the side wall, and to values closer to ε_{ryy} when the strip moves closer to the bottom wall. This behavior can be explained by the edge effect.

Characteristic impedance increases with moving the strip away from the shield towards the center of the structure, which is due to general decrease of the capacitance per unit length and is not directly associated with the anisotropy of the substrate.

Acknowledgement

This research was partly funded by the Serbian Ministry of science and technological development, under grant TR-32052.

References

[1] J. Jin, *The Finite Element Method in Electromagnetics*, Wiley:NewYork, 1993.

[2] P. P. Silvester, *Finite Elements for Electrical Engineers*, 3rd Ed., Cambridge University Press, 1996.

[3] V. V. Petrović, B. D. Popović, “Optimal FEM solutions of one-dimensional EM problems,” *International Journal of Numerical Modelling: Electronic Networks, Devices and Fields*, Vol. 14, No. 1, pp. 49–68, Jan-Feb 2001.

[4] Ž. J. Mančić and V. V. Petrovic, “Strong and Weak FEM Formulations of Higher Order for Quasi-Static Analysis of Shielded Planar Transmission Lines,” *Microwave and Optical Technology Letters*, Vol. 53, No. 5, pp. 1114–1119, May 2011.

[5] Ž. J. Mančić, S. R. Aleksić, Vladimir V. Petrović, “Comparison of FEM, MoM and EEM in Solving a Benchmark 2D Electrostatic Problem,” Proc. 8th International Conference On Applied Electromagnetics – PES 2007, Niš, Serbia, September 3–5, 2007.

[6] Z. J. Mancic, V. V. Petrovic, “Analiza kvadratnog koaksijalnog voda sa anizotropnim dielektrikom metodom konačnih elemenata,” Proc. XVIII Telekom. forum TELFOR, Belgrade, Serbia, November 2010, pp. 850–853 (in Serbian).

[7] V. V. Petrovic, Z. J. Mancic, “Strong FEM Formulation for Quasi-Static Analysis of Shielded Planar Transmission Lines in Anisotropic media,” 5th European Conference on Circuits and Systems for Communications (ECCSC'10), Belgrade, Serbia, November 2010, pp. 253–255.

[8] *Mathematica*, Ver.7, Wolfram Research, Inc., USA.